Journal of Materials and
Environmental Sciences
ISSN : 2028-2508
CODEN : JMESCN

J. Mater. Environ. Sci., 2020, Volume 11, Issue 1, Page 69-78

http://www.jmaterenvironsci.com

Recoverable Adsorbent of Natural Zeolite/Fe_3O_4 for Removal of Pb(II) in Water

T. Pambudi [1], E.T. Wahyuni [1*], and M. Mudasir [1]
[1]*Chemistry Department, Faculty of Mathematics and Natural Sciences, Gadjah Mada University*
Sekip Utara, P.O. Box Bls. 21, Yogyakarta 55281, Indonesia

Received 14 Oct 2019
Revised 01 Dec 2019
Accepted 03 Dec 2019

Keywords

- ✓ *Pb(II) ion*
- ✓ *Adsorption*
- ✓ *natural zeolite*
- ✓ *magnetization*

endang_triw@ugm.ac.id
Phone : +62274870052
Fax : +62544188

Abstract

A recoverable adsorbent of magnetized natural zeolite (zeolite-Fe_3O_4) has been prepared by two different techniques, named as co-precipitation and impregnation. The characters and the performance of the zeolite-Fe_3O_4 adsorbents prepared by the two of different techniques were compared. The performance of the adsorbents was evaluated for Pb(II) removal. In addition, the influence of the Fe_3O_4 fraction (25.0% w/w, 33.3% w/w, 50.0% w/w) on the adsorption capacity and recoverability was also studied. The adsorptions of Pb(II) was proceeded by batch experiment, where the operating parameters, including adsorbent mass, pH, and time were optimized. The adsorption kinetic and isotherm were also determined. The research results assign that zeolite-Fe_3O_4 prepared by co-precipitation has larger surface area, better Fe_3O_4 dispersion, higher recoverability, and considerably same adsorption capacity compared to that of by impregnation technique. Further, increasing Fe_3O_4 fraction can raise the recoverability, but leads to a decrease in the adsorption capacity. The 33.3%w/w fraction of Fe_3O_4 in the adsorbents give compromisingly good adsorption capacity and recoverability. The maximum of Pb(II) adsorption (95.15%) from 1 L solution with Pb(II) concentration of 150 mg L^{-1} is reached by using 1.25 g of the adsorbent mass, pH 3, and contact time 90 min. The adsorption kinetic best fits to pseudo second order with adsorption rate = 3.752 g mg^{-1} min^{-1}. The corresponding adsorption is well described by Langmuir isotherm model with adsorption capacity = 55.249 mg g^{-1}. The adsorption energy is found to be 31.548 kJ mol^{-1} suggesting that the adsorption follows the chemisorption phenomena.

1. Introduction

Zeolites have received considerable attention for contaminant removal due to their high adsorption capacity, low cost and worldwide abundance in case of natural zeolite [1]. Due to its superior properties, zeolites have been frequently used to remove various pollutants, such as phenol [2], dyes [3], and heavy metals [4]. Commonly techniques used to separate zeolite adsorbent after adsorption process were filtration and centrifugation, which is impractical, time-consuming and expensive on a large scale of adsorption [5]. These problems can be overcame by modifying the adsorbent to be magnetic, so that it can be separated easily and rapidly using a magnetic bar [5-12]. Synthesis of magnetic zeolites has been performed using co-precipitation method [5-8] and impregnation [9-12]. Co-precipitation is based on precipitation of Fe_3O_4 on zeolite surfaces using starting material of a mixture of Fe(II) and Fe(III) ions in the solution under alkaline conditions [5-8]. Meanwhile impregnation occurs through physically interacting between zeolite powder suspended in water and Fe_3O_4 powder under constant stirring [9-12]. It was reported that the two techniques resulted in good recoverability adsorbents

Although the two different techniques have been occasionally used for magnetization of zeolites, to best of our knowledge the comparison of the characters and adsorption capacity of the magnetic zeolite adsorbents prepared by co-precipitation to that of prepared by impregnation, has not been published. By comparing their characters and adsorption capacity, we will find which method resulting better characters and adsorption capacity, that further can be recommended to be applied in industries. Under the circumstance, in this present paper we addressed the comparison of the characters and adsorption ability of magnetic Indonesian natural zeolite adsorbents prepared by the two different techniques. The adsorption capacity of the magnetic natural zeolite was evaluated by adsorption of Pb(II) ion in the solution.

Pb(II) ion was chosen for examining adsorption capacity of the magnetic zeolite adsorbent, since Pb(II) is a heavy metal that is widely distributed in the environment and tends to accumulate that causes numerous diseases [13-14]. The chronic effects of Pb are characterized by several diseases such as nerve paralysis, kidney inflammation, anemia, and increasing uric acid in the blood [13]. The major resources of lead pollution in the aquatic are waste water of metal coating facilities, mining, battery manufacturing, paint/pigment production, and glass production industries [14-15]. In order to prevent of Pb(II) contamination in water, elimination of Pb(II) to reach permissible level is urgent to be carried out. Decreasing Pb(II) concentration in water has been currently studied by adsorption method, using a numerous of adsorbents [13-19], because it is an effective, economical, and flexible in design and operation method. However, adsorption of Pb(II) by using magnetic Indonesian natural zeolite has not been explored yet. In this study, we also evaluate the effect of the operating parameters such as adsorbent dose, contact time, solution pH, and initial Pb(II) concentration on the effectiveness of Pb(II) adsorption. Further, the adsorption kinetic parameters are also determined.

2. Material and Methods

2.1. Materials and instruments

Natural zeolite from Bayat, Klaten, Central Java, Indonesia was used as an object to research. Chemicals used in this research were $FeCl_3{\cdot}6H_2O$, $FeCl_2{\cdot}4H_2O$, $Pb(NO_3)_2$, Pb(II) standard solution 1000 mg L^{-1}, HCl 36% , NaOH Pellet 99.90% of the purity, NH_4OH solution 25%, that were purchased from E.Merck. company. JEOL JSM-6510LA of Scanning Electron Microscopy, Shimadzu 8201 PC FTIR spectrophotometer, BELSORP-mini device surface area analyzer, 2020 Lamotte Turbidimeter, and 3110 Perkin-Elmer-AAS machines, were operated for analysis and characterizations.

2.2. Procedures

2.2.1. Magnetization of natural zeolite

2.2.1.1. By co-precipitation

As much as 1.5 g of washed zeolite was suspended in 400 mL NH_3 solution 0.5 mole L^{-1}. The suspension was stirred under the constant rate and N_2 flowing to get well-homogeneous, and then it was heated at 70°C for 30 min. Into the suspension, 100 mL of a solution containing Fe(II) and Fe(III) ions with a molarity ratio of 1:2 was added gradually, so that the black solid of zeolite-Fe_3O_4 was formed. The black solid then was separated using magnetic bar, washed using deionized water until neutral pH, and dried at 80°C. The black solid of zeolite-Fe_3O_4 contained 50.00% w/w of Fe_3O_4 fraction. The procedure was repeated for preparation of zeolite-Fe_3O_4 with 33.30% w/w and 25.00% w/w Fe_3O_4 fractions by changing the zeolite mass, that were as 3.0 g and 4.5 g, respectively. The black solids were coded as zeolite-$Fe_3O_{4(p\text{-}50)}$, zeolite-$Fe_3O_{4(p\text{-}33)}$, and zeolite-$Fe_3O_{4(p\text{-}25)}$ representing the technique used and Fe_30_4 fraction. Then the zeolite-Fe_3O_4 samples were grinded and sieved using a 250 mesh sieve and were ready for characterization and adsorption experiment.

2.2.1.2. By Impregnation technique

The washed zeolite as much as 0.5 g of was suspended in 40 mL of deionized water, accompanied with the constant stirring to get well-homogeneous suspension, under the N_2 gas atmosphere. Then 0.5 g of Fe_3O_4 powder was added gradually into the zeolite suspension under constant stirring to form homogeneous mixture and was left for 1 hour. The black solid formed of zeolite- Fe_3O_4 was separated from the solvent by using magnetic bar and dried at 80°C. The black solid was presented as zeolite-Fe_3O_4 with 50.0% w/w Fe_3O_4 fraction. Then the solid was grinded and sieved using a 250 mesh sieve. The procedure was copied for preparation of zeolite-Fe_3O_4 adsorbents possessing 33.3% w/w and 25.0% w/w of Fe_3O_4 fractions, by changing the zeolite weights, that were 1.0 g and 1.5 g. The adsorbents were coded as Zeolite-$Fe_3O_{4(i\text{-}50)}$, Zeolite-$Fe_3O_{4(i\text{-}33)}$ Zeolite-$Fe_3O_{4(i\text{-}25)}$ following the technique used and the fraction of Fe_3O_4.

2.2.2. Adsorption of Pb(II) in the solution

Pb(II) adsorption by zeolite-Fe_3O_4 adsorbent was carried out in batch experiment, following procedure : 100 mL of Pb(II) solution with concentration of 150 mg L^{-1} was added with 12.5 mg of zeolite-$Fe_3O_{4(p\text{-}50)}$ adsorbent. Then the mixture was stirred under constant rate for 30 min. The adsorbent was recovered by magnetic bar, and the filtrated was analyzed by AAS to determine Pb(II) concentration left in the solution. The same procedure was used for different adsorbents of zeolite-$Fe_3O_{4(p\text{-}33)}$ and zeolite-$Fe_3O_{4(p\text{-}25)}$ as well as for zeolite-$Fe_3O_{4(i\text{-}50)}$, zeolite-$Fe_3O_{4(i\text{-}33)}$, and zeolite-$Fe_3O_{4(i\text{-}25)}$. From the various adsorbents, it would be found the best adsorbent, then it was used for adsorption with various dosage (2.5 mg -15.0 mg in 100 mL), solution pH (2-6), contact time (5–180 min) and initial Pb(II) concentrations (25–300 mg L^{-1}). The pH of the solution was adjusted by adding 0.1 mole

L^{-1} NaOH to reach higher pH, or by addition of 0.1 mole L^{-1} HCl to decrease the pH as desired, that was maintained with the corresponding buffers. The adsorption efficiency represented as R(%) was calculated using equation (1) below:

$$R = \frac{C_0 - C_e}{C_0} \times 100\% \qquad (1)$$

Then the adsorption capacity presented as Q_e (in mg g^{-1}) was calculated using equation (2)

$$Qe = \frac{(C_0 - C_e)V}{W}. \qquad (2)$$

Where, C_0 and C_e were the initial and final Pb(II) concentrations (mg L^{-1}) respectively, V was the volume of Pb(II) solution (L), and W was the adsorbent dose (g).

3. Result And Discussion

3.1. Effect of preparation techniques and Fe_3O_4 fraction on the adsorbent characters

3.1.1. The surface characters

The surface characters including pore diameters, surface area, and pore volume of the adsorbents prepared by two different techniques with various Fe_3O_4 fractions are displayed in Table 1. The table shows that the magnetization can decrease the pore diameters, but improves the surface area and pore volumes. Decreasing the pore diameter may be due to the filling Fe_3O_4 particles in the zeolite pores. Such reason is supported by the fact that increasing Fe_3O_4 fraction gives smaller pore diameter, because more Fe_3O_4 particles have blocked the pores. The improvement of the surface area indicates that Fe_3O_4 particles also provide surface active into the adsorbents. This is consistence with the data in the table showing that more Fe_3O_4 loaded in the adsorbent contributes larger surface area, but further increase of Fe_3O_4 may form aggregate with larger size that declines the surface area. The additional of the pore volume may be created by Fe_3O_4 particles that is well dispersed and aggregated [18].

Table 1. Surface and pore properties of the adsorbents prepared

Adsorbent	d_{BET} (nm)	S_{BET} (m^2 g^{-1})	V_m (cm^3g^{-1})
Un-magnetic zeolite	18.67	21.20	0.0989
Zeolite-$Fe_3O_{4(p-50)}$	13.58	77.68	0.1454
Zeolite-$Fe_3O_{4(p-33)}$	10.07	88.14	0.2219
Zeolite-$Fe_3O_{4(p-25)}$	7.39	78.69	0.2637
Zeolite-$Fe_3O_{4(i-50)}$	11.54	68.79	0.1395
Zeolite-$Fe_3O_{4(i-33)}$	11.36	75.76	0.1584
Zeolite-$Fe_3O_{4(i-25)}$	9.55	58.40	0.1984

Additionally, it is also observable that the surface and pore characters of the adsorbents prepared by co-precipitation are better than that of the one prepared by impregnation. The possible reason is that by co-precipitation technique, the interaction between zeolite powder with the Fe(II) and Fe(III) ions to form Fe_3O_4 precipitate might proceed homogenously, and so resulted in the better Fe_3O_4 dispersion on the zeolite structure. Meanwhile in the impregnation technique, the Fe_3O_4 and the zeolite powders only mixed physically , that gave less dispersion of Fe_3O_4 particles.

3.1.2 SEM images

The SEM images were scanned to find out the distribution of Fe_3O_4 on the zeolite structure, that are displayed as figure 1. In general, the figure probes that smaller particles, that must be Fe_3O_4, cover the larger particles of zeolites. The increase of Fe_3O_4 fraction, more particles of Fe_3O_4 with larger size are dispersed on the zeolite surface. Further, it is also demonstrated that smaller particles of Fe_3O_4 with better dispersion is found in zeolite-Fe_3O_4 prepared by co-precipitation, compared to that of from the impregnation technique. This contrary appearance can occur because Fe_3O_4 from co-precipitation from Fe^{2+} and Fe^{3+} in the solution may interact strongly with the zeolite structure [18], that inhibited the particle growth of the Fe_3O_4 particles resulting smaller and better dispersion, that might not happen in the impregnation method.

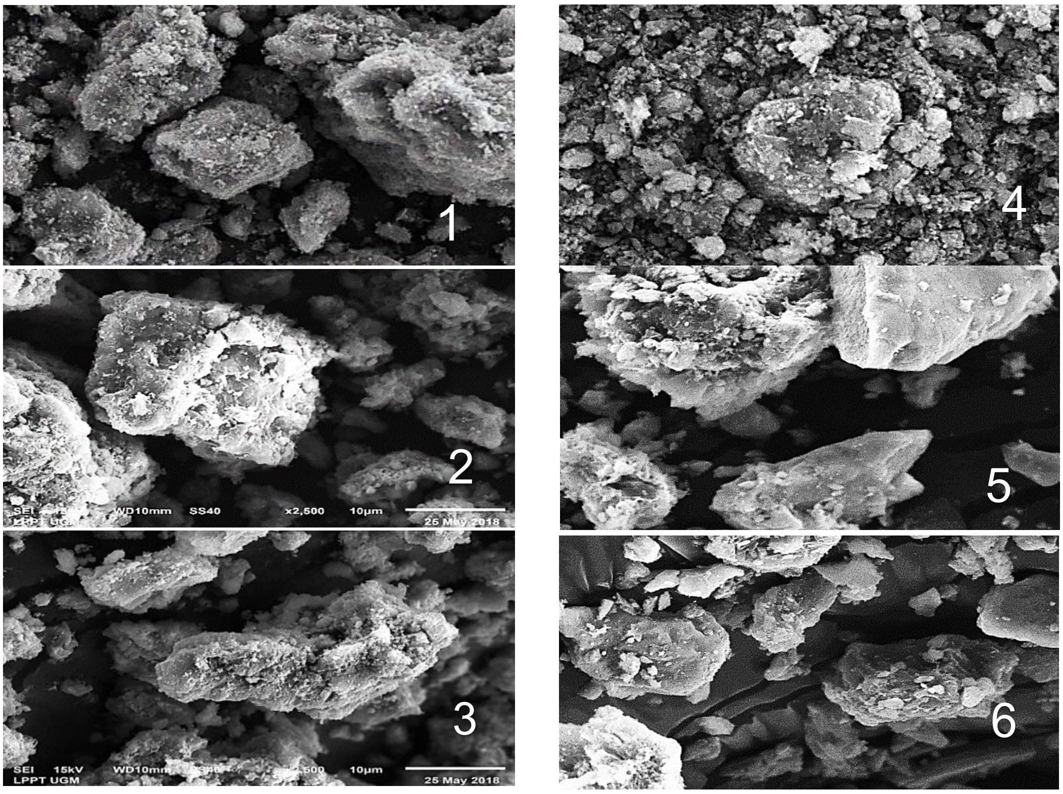

Figure 1 : The SEM images of 1) Zeolite-$Fe_3O_{4(p\text{-}25)}$, 2) Zeolite-$Fe_3O_{4(p\text{-}33)}$, 3) Zeolite-$Fe_3O_{4(p\text{-}50)}$, 4) Zeolite-$Fe_3O_{4(i\text{-}25)}$, 5) Zeolite-$Fe_3O_{4(i\text{-}33)}$, and 6) Zeolite-$Fe_3O_{4(i\text{-}50)}$

3.1.3. Infra Red spectra

To detect the interaction between Fe_3O_4 with the zeolite structure that may be happened, their IR spectra have been recorded, as seen in figure 2. From the spectra it can be seen that several characteristic peaks of zeolite appear at 3425, 3441, 1635, 1049, 462 and 447 cm^{-1} of the wavenumbers. Absorption band at 3425-3441 cm^{-1} region represents stretching vibration of O-H bonds of water molecules in zeolites. This band is overlap with the stretching vibration of the O-H bonds of hydroxyl terminal group in zeolite [18]. Absorption band at 1635 cm^{-1} indicates the bending vibration of the H–O–H bond from water.

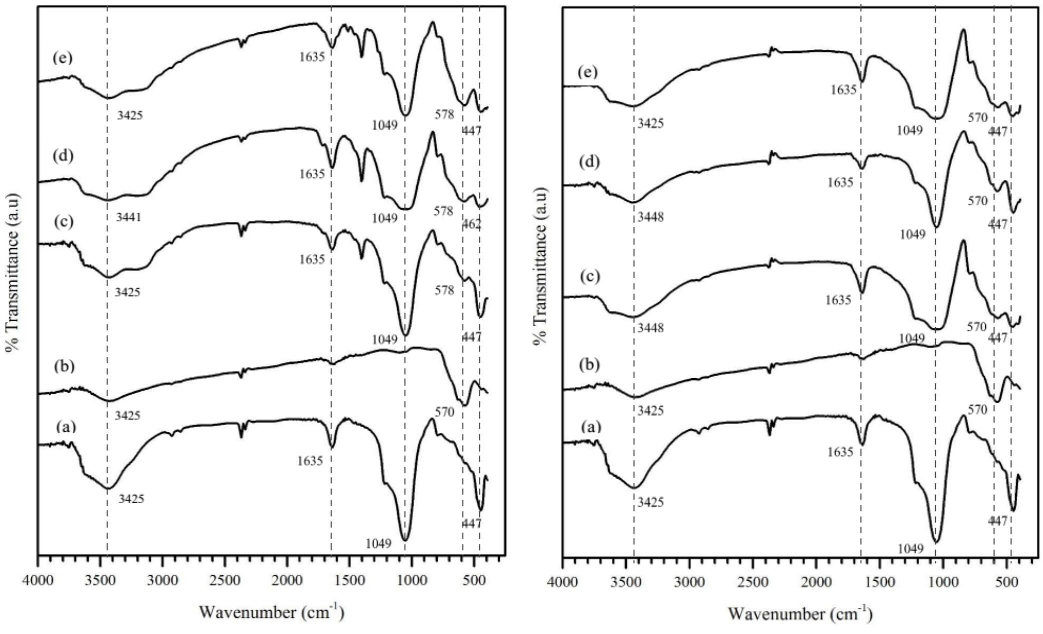

(A) (B)

Figure. 2: IR spectra A represents a) Zeolite, b) Fe_3O_4, c) zeolite-$Fe_3O_{4(p\text{-}25)}$, d) zeolite-$Fe_3O_{4(p\text{-}33)}$, e) zeolite-$Fe_3O_{4(p\text{-}50)}$. IR spectra B represents a) Zeolite, b) Fe_3O_4, c) zeolite-$Fe_3O_{4(i\text{-}25)}$, d) zeolite-$Fe_3O_{4(i\text{-}33)}$, e) zeolite-$Fe_3O_{4(i\text{-}50)}$.

Sharp and strong absorption band at 1049 cm^{-1} correspond to O-Si-O/O-Al-O asymmetry stretching while the absorption band at 447-462 cm^{-1} region is due to the presence of the bending vibration of O-Si-O/O-Al-O bonds in the tetrahedral framework of zeolite [18]. Fe_3O_4 has characteristic absorption peaks of 3425 and 570 cm^{-1} assigning to O-H and Fe-O bond vibrations, respectively [20]. Moreover, the absorption peaks of all zeolite-Fe_3O_4 adsorbents prepared from the two different techniques are seen as combination peaks of zeolite and Fe_3O_4. It is suggested that Fe_3O_4 particles have coated the zeolite structure. In the spectra of zeolite- Fe_3O_4 adsorbent prepared by co-precipitation, a new peak at around 1425 cm^{-1} is observed, that is not seen in the spectra of the respective adsorbent prepared by impregnation technique. The new peak is believed to be contributed by Fe-O-Si bond [18]. It implies that co-precipitation allowing Fe atoms of Fe_3O_4 to be attached with Si-O of the zeolite, indicating the successful coating of Fe_3O_4 particles on the zeolite surface. The absence of the new peak in the adsorbents from the impregnation technique indicates that there is no chemical interaction between Fe_3O_4 and the natural zeolite. This data well agrees with the SEM images presented above.

3.1.4. Recoverability qualitatively

The solutions separated magnetically from the zeolite-Fe_3O_4 adsorbents were displayed in figure 3. The figure attributes that increasing fraction of Fe_3O_4 in the adsorbents tends to enhance the clarity of the filtrate, referring the improvement of the adsorbent recoverability. It is confirmed that the recoverability of the adsorbent is contributed by Fe_3O_4 possessing magnet property. Additionally, the corresponding solutions from zeolite-Fe_3O_4 prepared by co-precipitation are clearer than that of by impregnation, assigning that the corresponding adsorbents have better recoverability. The better recoverability of the zeolite-Fe_3O_4 should be due to the better dispersion of Fe_3O_4 on the zeolite surface as proven by SEM images.

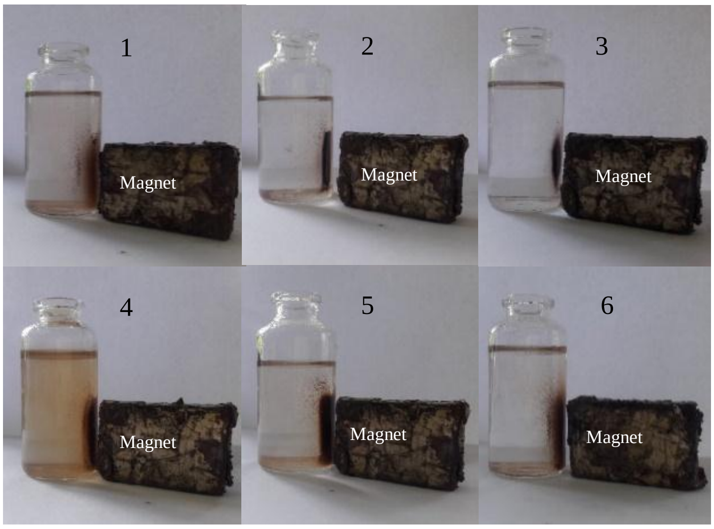

Figure 3: Clarity of the filtrates separated from : 1) zeolite-$Fe_3O_{4(p\text{-}25)}$, 2) zeolite-$Fe_3O_{4(p\text{-}33)}$, 3) zeolite-$Fe_3O_{4(p\text{-}50)}$, 4) zeolite-$Fe_3O_{4(i\text{-}25)}$, 5) zeolite-$Fe_3O_{4(i\text{-}33)}$, and 6) zeolite-$Fe_3O_{4(i\text{-}50)}$

3.1.5. Adsorption capacity and recoverability quantitatively

Other characters of the adsorbents are adsorption capacity and recoverability. Figure 4 shows the adsorption ability of the adsorbents and turbidity of the filtrates resulted from the separation of the corresponding adsorbents prepared two different techniques. It takes to note that higher turbidity represents lower clarity of the filtrate, further it illustrates the lesser recoverability of the corresponding adsorbent. The figure indicates that increasing Fe_3O_4 fraction in the adsorbents, has raised the recoverability, but in contrast it causes the adsorption capacity slightly declined. The presence of Fe_3O_4 can contribute the magnetic property on the adsorbents, allowing them easier to be recovered magnetically. At the same time, the particles of Fe_3O_4 also cover some part of the zeolite surface that reduced the adsorption active sites. It is clear that although Fe_3O_4 can extent the surface area of the adsorbents , but it does not always enlarge the adsorption surface. It is also observable that zeolite-Fe_3O_4 from co-precipitation technique has higher recoverability with equal adsorption effectiveness compared to the one prepared by impregnation. The better recoverability is created by the better dispersion of Fe_3O_4 on the adsorbent, as discussed above. It is clear that this data is in a good agreement with the clarity appearance.

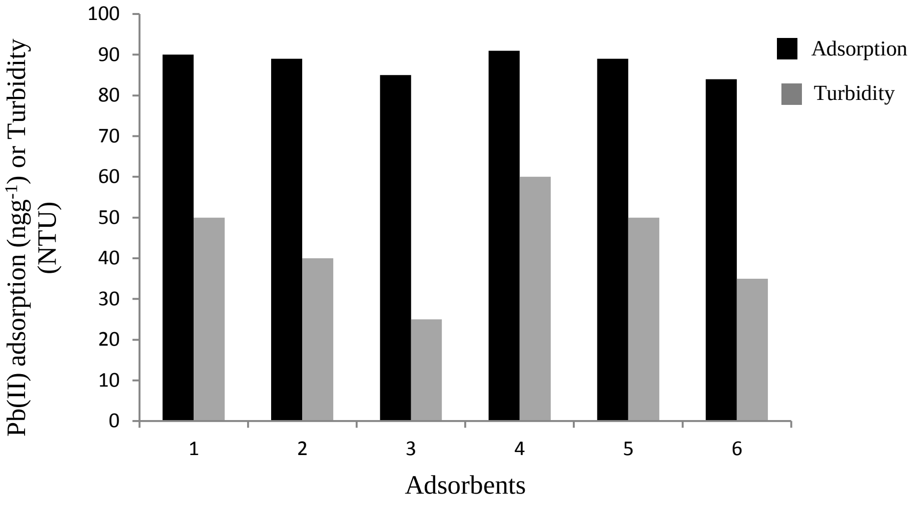

Figure 4: The adsorption capacity and turbidity of 1) zeolite-$Fe_3O_{4(p\text{-}25)}$, 2) zeolite-$Fe_3O_{4(p\text{-}33)}$, 3) zeolite-$Fe_3O_{4(p\text{-}50)}$, 4) zeolite-$Fe_3O_{4(i\text{-}25)}$, 5) zeolite-$Fe_3O_{4(i\text{-}33)}$, and 6) zeolite-$Fe_3O_{4(i\text{-}50)}$

3.2. The adsorption of Pb(II) by the recoverable adsorbents

For the adsorption evaluation, the adsorbents studied are zeolite-Fe_3O_4 prepared by co-precipitation with various Fe_3O_4 fractions, since the adsorbents show better characters as presented above.

3.2.1. Effect of adsorbent doses

Fig.5 shows the effect of the adsorbent dose on the adsorption of Pb(II) ions. From the figure it can be seen that the increase of the adsorbent dose can improve the effectiveness of Pb(II) adsorption and the maximum effectiveness is reached by 0.75 g L^{-1} of the dose. It is because the more amount of the adsorbent, the larger adsorption active sites are provided. Similar finding has also been reported [11]. The adsorption effectiveness does not depend on the adsorbent dose when it is higher than 0.75 g L^{-1}, because all Pb(II) has been adsorbed, so that no Pb(II) left in the solution.

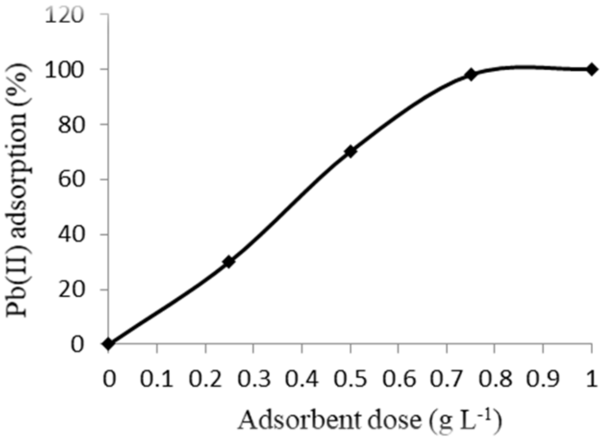

Figure 5: The effect of the adsorbent dose on the Pb(II) adsorption

3.2.2. Effect of pH

The effect of the solution pH on the Pb(II) adsorption is displayed in figure 6. The figure indicates that increasing pH up to 3, the effectiveness of the adsorption enhances sharply but it reduces when the pH is elevated up to 6. At low pH, the H^+ concentration is very high allowing it to compete with Pb^{2+} in the adsorption, that leads to the low adsorption [14]. Increasing pH, where the number of H^+ is reduced, may decrease the competition, that promotes more Pb(II) adsorption. When the pH is further increased, more number of OH^- available that can react with some Pb^{2+} ions to form $Pb(OH)^+$ that declines the number of Pb^{2+} to be adsorbed [14].

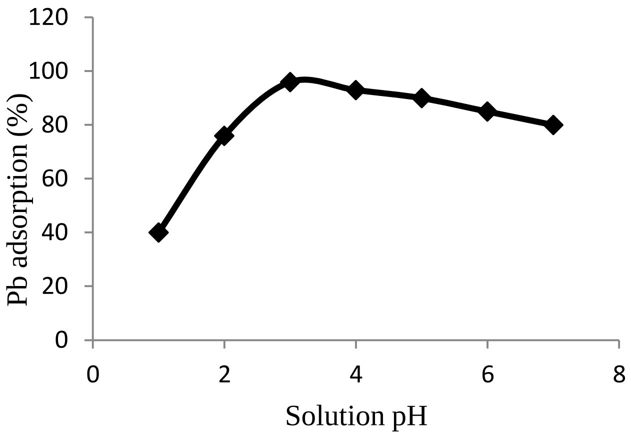

Figure 6: The effect of solution pH on the Pb(II) adsorption

3.2.3. Effect of contact time

The effect of contact time on the adsorption of Pb(II) ions is shown in figure 7. It can be observed that the adsorption increases with the extension contact time. The initial rapid uptake can be explained by the presence of large number of vacant sites on the adsorbent surface. As the time proceeds, the adsorption effectiveness reaches a constant value beyond which no more Pb(II) ion can occupy the active sites. This is due to the fully occupation of Pb(II) ion the vacant sites [13-15]. The equilibrium was reached rapidly after 30 min, that may be interesting for practical application of adsorption in wastewater treatment.

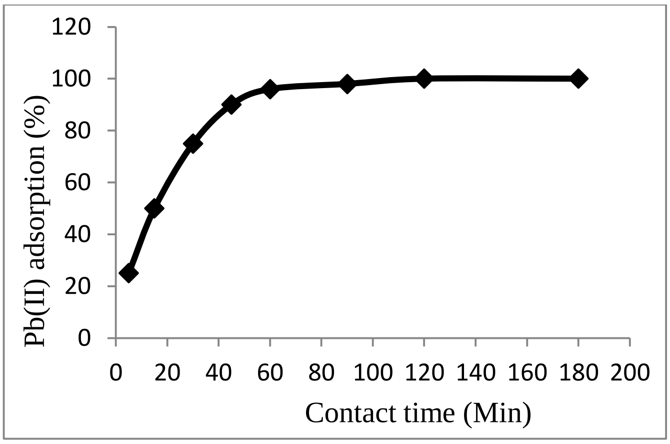

Figure 7 : The effect of the contact time on the Pb(II) adsorption

3.2.4. Effect of initial concentration of Pb(II)

Figure 8 shows the effect of the initial concentration of Pb(II) ion on the adsorption effectiveness. The figure attributes that increasing the initial concentration of Pb(II) ions promotes more adsorption, since the interaction between Pb(II) with the zeolite surface takes place effectively.

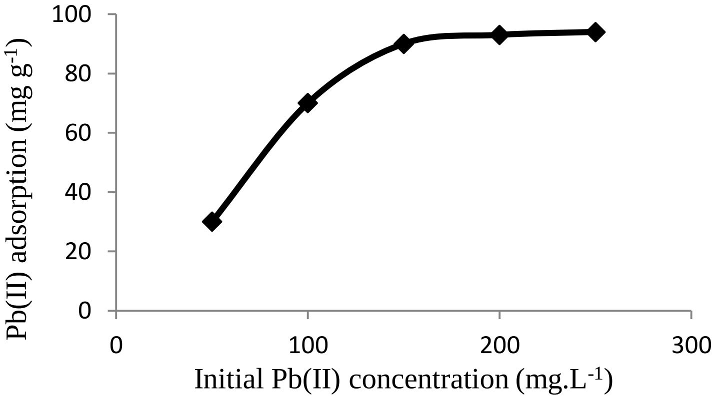

Figure 8: The effect of the initial Pb(II) concentration on the adsorption

However, when the initial Pb(II) concentration higher than 150 mg L^{-1} the adsorption can be not improved because the surface of the adsorbent may be fully occupied by Pb(II) ions [13, 15]. Consequently, no place in the zeolite surface for the left Pb(II) in the solution.

3.2.5. Adsorption kinetic and isotherm studies

Adsorption kinetic parameters were determined based on the data of the contact time variation by following equations for pseudo-first order and pseudo-second order [15]. The parameters obtained were adsorption capacity at equilibrium (q_e) and adsorption rate constant (k), that were presented in Table 2. It shows that the adsorption kinetics of Pb(II) ions well fits with the pseudo second-order model as indicated by R^2 (correlation coefficient) as much as 0.999. Some studies found same results [14-15]. These results are also reinforced by reports that most adsorption of divalent metal follows the pseudo second-order kinetics model [21]. Pseudo second-order model represents that the rate controlling step for the adsorption involves chemical reactions or chemisorption [14] by covalent forces or ion exchange between the adsorbent with Pb(II) ions [15]. The adsorption capacity is found to be 27.472 mg g^{-1} with the adsorption rate constant of 3.752 g mg^{-1} min^{-1} that show good ability of the adsorbent and promising potential to industry application.

Table 2: The adsorption kinetic parameters

Pseudo first order Lagergren			Pseudo second order Ho		
q_e (mg g^{-1})	k_1 (min^{-1})	R^2	q_e (mg g^{-1})	k_2 (g mg^{-1} min^{-1})	R^2
0.935	9.21×10^{-3}	0.343	27.472	3.752	0.999

The adsorption isotherm model was approached based on the data of the initial concentration. By plotting the data into the equations for Langmuir and Freundlich models [14-15, 21], some parameters could be obtained, as displayed in Table 3. In Langmuir isotherm model, q_{max}-(mg g^{-1}) is the Langmuir monolayer adsorption capacity and b (L mg^{-1}) is the Langmuir adsorption intensity constant as the ratio of the adsorption rate to the desorption rate, indicating the solid surface affinity and ability [14]. Meanwhile in Freundlich isotherm model, K_f (mg g^{-1}) is the Freundlich isotherm constant representing the adsorption capacity and n_f is the adsorption intensity, reflecting the degree of difficulty for adsorption. When n exceeds 2 but no more than 10, the adsorption process is easy to proceed. Comparatively, the ability for adsorption will be too weak when n is less than 0.5 [14].

Table 3: The adsorption isotherm

Isotherm Langmuir			**Isotherm Freundlich**		
q_{max} (mg g^{-1})	b (L mg^{-1})	R^2	K_f (mg g^{-1})	n_f	R^2
55.249	1.382	0.966	27.146	5.336	0.888

Table 3 probes the correlation of the Langmuir model of the Pb(II) adsorption is 0.999, confirming that the adsorption follows the Langmuir isotherm. It suggest the monolayer adsorbed Pb(II) ion is formed on the surface of the adsorbent. The adsorption capacity of Pb(II) is 55.249 mg g^{-1}. The adsorption energy is found as 31.548 kJ mol^{-1}, that suggests the chemisorption. The same finding were also obtained and reported previously [14-15, 21] through interactions between Pb^{2+} ions and silanol groups or aluminol of zeolites [11, 18].

Conclusion

Adsorbents of zeolite-Fe_3O_4 prepared by co-precipitation possess better characters with respect to the surface characters and recoverability compared to the adsorbent prepared by impregnation technique. Further, increasing Fe_3O_4 fraction in the adsorbents can enhance the recoverability but at the same time it decreases the adsorption capacity. The medium fraction of Fe_3O_4 (33.30%w) in the adsorbent shows the best compromise of adsorption capacity and recoverability. From the adsorption study it is found that the adsorption of Pb(II) with concentration of 150 mg L^{-1} by zeolite-Fe_3O_4 $_{(p-33)}$ can reach maximum effectiveness (95.15%) by applying 1.25 g L^{-1} of the adsorbent dose, pH 3, and 90 min of the contact time. The adsorption of Pb(II) ions on the adsorbent is well fitted to pseudo second-order model with reaction rate constant of 3.752 g mg^{-1} min^{-1}. The corresponding adsorption is in a good agreement with Langmuir isotherm model with adsorption capacity of 55.249 $mg.g^{-1}$. The adsorption energy is found to be 31.548 $kJ.mol^{-1}$ suggesting the chemisorption mechanism.

Acknowledgement

A great acknowledgment to Universitas Gadjah Mada for the financial support in conducting this research through RTA schema Project Grant with the Contract No. 3194/UN1/DITLIT/DIT-LIT/LT/2019, April 11 2019.

References

1. M. Karatas, Removal of Pb(II) from Water by Natural Zeolitic Tuff: Kinetics and Thermodynamics, *J. Hazard Mater*. 199–200 (2012) 383–389.
2. M. Khalid, G. Joly, A. Renaud, P. Magnoux, Removal of Phenol from Water by Adsorption Using Zeolites, I*nd. Eng. Chem. Res.* 4317 (2004) 5275-5280. https://doi.org/10.1021/ie0400447
3. V. Hernández-Montoya, M. A. Pérez-Cruz, D. I. Mendoza-Castillo, M. R. Moreno-Virgen,A. Bonilla-Petriciolet, Competitive adsorption of dyes and heavy metals on zeolititc Structures, *J. Environ. Man.* 116 ((2013) 213-222. https://doi.org/10.1016/j.jenvman.2012.12.010.
4. T.P. Belova, Adsorption of heavy metal ions (Cu^{2+}, Ni^{2+}, Co^{2+} and Fe^{2+}) from aqueous solutions by natural zeolite, . *Heliyon,* 5(9) (2019) e02320.
5. S.M. Bello, R.A. M. Luckie, L. F. Santos, J. P. Hinestroza, V.S. Mendieta, Size-controlled Synthesis of Fe_2O_3 and Fe_3O_4 Nanoparticles onto Zeolite by Means of a Modified Activated-Co-precipitation Method: Effect of the HCl Concentration During the Activation, *J. Nanopart. Res.*, 14 (2012) 1242-
6. N. H. Mthombeni, M. S. Onyango, O. Aoyi, Adsorption of Hexavalent Chromium onto Magnetic Natural Zeolite-Polymer Composite, *J. Taiwan. Inst. Chem. Eng.*, 50 (2015) 242–251.
7. A. Mohseni-Bandpi T.J. Al-Musawi, R. Ghahramani, Z. Zarrabi, S. Mohebi S, A. Vahe. Improvement of zeolite adsorption capacity for cephalexin by coating with magnetic Fe_3O_4 nanoparticles. *J. Taiwan. Inst. Chem. Eng*., 218 (2016) 615–624
8. A. Mesdaghinia, A. Azari, R. N. Nodehi, K. Yaghmaeian, A. K. Bharti, S. Agarwal, V.K. Gupta, K. Sharafic, Removal of Phthalate Esters (PAEs) by Zeolite/Fe_3O_4: Investigation on the Magnetic Adsorption Separation, Catalytic Degradation and Toxicity Bioassay, *J. Mol. Liq.,* 233 (2017) 378 –390.
9. I.W. Nah, K. Y. Hwang, Y.G. Shul, A Simple Synthesis of Magnetically Modified Zeolite, *Powder Technol*., 177 (2007) 99-101.
10. H. Liu, S. Peng, L. Shu, T. Chen, T. Bao, R. L. Frost. Magnetic zeolite NaA: Synthesis, characterization based on metakaolin and its application for the removal of Cu^{2+}, Pb^{2+}, *Chemosphere.* 91 (2015) 1539–1546
11. M. Yuan, T. Xie, G. Yan, Q. Chen, L. Wang, Effective removal of $Pb^{2+}$from aqueous solutions by magnetically modified zeolite, *Powder Technol*., 332 (2018) 234–241.
12. C. Jilin, C. Guihuan, G. Hongfei, C. Jianxin, Synthesis and Characterization of Magnetic ZSM-5 Zeolite. *Trans. Tianjin Univ*. 19 (2013) 326-331. DOI 10.1007/s12209-013-1912-0
13. A.M. Soliman, M.E. Hanan, T. Thiemann, Y. Majedi, F. T. Labata, N.A.F. Al-Rawashdeh, Removal of Pb(II) ions from aqueous solutions by sulphuric acid-treated *palm tree* leaves. *J. Taiwan. Inst. Chem. Eng.,* 58 (2016) 264–273
14. S. Yao, J. Zhang, D. Shen, R. Xiao, S. Gu, M. Zhao, J. Liang, Removal of Pb(II) from water by the activated carbon modified by nitric acid under microwave heating. *J. Colloid Interface Sc*., 463 (2016) 118–127
15. X. Li, W. Zheng, D. Wang, Q. Yang, J. Cao, X. Yue, T. Shen, G. Zeng, Removal of Pb (II) from aqueous solutions by adsorption onto modified areca waste: Kinetic and thermodynamic studies. *Desalination* 258 (2010) 148–153.
16. E.T . Wahyuni, M. Mudasir, Improvement of Ion-Exchange Capacity of Indonesian Natural Zeolite by Sequential Washing Using Hydrofluoric Acid and EDTA Solutions, *J. Ion Exchange*, 18 (2007) 196-201

17. M. E. Mahmoud, A. E. H. Abdou, S. B. Ahmed, Conversion of Waste Styrofoam into Engineered Adsorbents for Efficient Removal of Cadmium, Lead and Mercury from Water. *ACS Sustainable Chem. Eng*. 4 (2016) 819-827. DOI: 10.1021/acssuschemeng.5b01149
18. M. Khodadadi, A. Malekpour, M. Ansaritabar, Removal of Pb(II) and Cu(II) from Aqueous Solutions by NaA Zeolite Coated Magnetic Nanoparticles and Optimization of Method using Experimental Design, *Microporous Mesoporous Mater*., 248 (2017) 256-265.
19. H. Chen, J. Zhao, G. Dai, J. Wu, H. Yan. Adsorption characteristics of Pb(II) from aqueous solution onto a natural biosorbent fallen Cinnamomum camphora leaves, *Desalination* 262 (2010) 174–182
20. F. Toubi, A. Deezagi, G. Singh, M.A. Oghabian, S. Safa**, A.** Fatemi, A. Arpanaei, Preparation and Characterization of Double Shell Fe_3O_4 Cluster@Nonporous SiO_2@Mesoporous SiO_2 Nanocomposite Spheres and Investigation of their In Vitro Biocompatibility, *Iran J Biotech.*, 13(1), (2015) e1068 DOI:10.15171/ijb.1068
21. E. Asuquo, A. Martin, P. Nzerem, F. Siperstein, X. Fan. Adsorption of Cd(II) and Pb(II) ions from aqueous solutions using mesoporous activated carbon adsorbent: Equilibrium, kinetics and characterization studies, *J. Environ. Chem. Eng*. 5 (2017) 679–698.

(2020) ; http://www.jmaterenvironsci.com